Published by IOP Publishing for Sissa Medialab

Received: *July 16, 2019*
Revised: *October 1, 2019*
Accepted: *January 19, 2020*
Published: *February 18, 2020*

Characterization of the efficiency of a cubic NaI detector with rectangular cavity for axially positioned sources

M.S. Badawi,[a] **S. Noureddine,**[b] **Y.N. Kopatch,**[c] **M.I. Abbas,**[d] **I.N. Ruskov,**[c,e] **D.N. Grozdanov,**[c,e] **A.A. Thabet,**[f] **N.A. Fedorov,**[c,g] **M.M. Gouda,**[d] **C. Hramco,**[c,h] **M. Abd-Elzaher,**[i] **A. Hamzawy,**[j] **M. Elsafi**[d,1] **and A.M. El-Khatib**[d]

[a] *Physics Department, Faculty of Science, Beirut Arab University, Beirut, Lebanon*
[b] *Physics Department, Faculty of Science, Lebanese University, Beirut, Lebanon*
[c] *Joint Institute for Nuclear Research (JINR), Dubna, Russia*
[d] *Physics Department, Faculty of Science, Alexandria University, 21511 Alexandria, Egypt*
[e] *Institute for Nuclear Research and Nuclear Energy (INRNE), BAS, Sofia, Bulgaria*
[f] *Department of Medical Equipment Technology, Faculty of Allied Medical Sciences, Pharos University in Alexandria, Egypt*
[g] *Faculty of Physics, Lomonosov Moscow State University (MSU), Moscow, Russia*
[h] *Institute of Chemistry, Academy of Science of Moldova, Chisinau, Republic of Moldova*
[i] *Department of Basic and Applied Sciences, Faculty of Engineering, Arab Academy for Science, Technology and Maritime Transport, Alexandria, Egypt*
[j] *Physics Department, Al-Jamoum University College, Umm Al-Qura University, Al-Jamoum, Saudi Arabia*

E-mail: mohamedelsafi68@gmail.com

Abstract: Scintillation NaI(Tl) crystals are typically utilized at room temperature for detection of energetic photons in high energy and nuclear physics research, non-destructive analysis of materials testing, safeguards, verification of nuclear treaty, geological exploration and therapeutic imaging. The present work provides a new geometry for the source-to-detector combination. A special order cubic detector with rectangular cavity was used. The mathematical expressions of the path-lengths traveled by the incident photon as well as the geometrical solid angle were derived. The detector efficiency was determined for an axially positioned standard point-like gamma-ray source using the analytical efficiency transfer technique. Geant4 Monte Carlo simulation code was also used to predict the detector response under the calibration geometry. The analytical efficiency transfer and Geant4 simulation results were compared with those obtained experimentally and a good agreement between them was shown.

Keywords: Imaging spectroscopy; Radiation-induced secondary-electron emission

[1]Corresponding author.

https://doi.org/10.1088/1748-0221/15/02/P02013

2020 JINST 15 P02013

Contents

2020 JINST 15 P02013

1 Introduction

Experimental determination of detector efficiency is considered to be a difficult and time-consuming process. That is why different computing methods are often used, such as: semi-empirical methods, Monte Carlo simulations, direct mathematical method and efficiency transfer method. Moens et al. [1] describe the principle of the semi-empirical methods, but for general use they are usually not accessible. The source-detector geometries are also limited, because some simplifications and approximations are used for their computation [1, 2].

The Monte Carlo simulation is used to determine the full-energy peak efficiency by using all related physical processes, which are occurring along the path of a photon, emitted from the source [3]. The first version of Geant was developed at CERN in 1974, The simulation of travelling particles through matter was done first by Geant3 Monte Carlo code. Some problems that appeared in Geant3 were tackled in Geant4 in 1994 [4]. The largest disadvantage of Monte Carlo simulation is that it needs a large number of primary photons (up to 10^7 photons) to obtain an uncertainty less than 1%, so it needs a long time for doing these calculations.

Selim and Abbas [5–7] proposed a direct mathematical method that is simple, direct, depends only on the geometrical parameter substitution of the source-to-detector system and the attenuation-coefficients μ of the incident photon, corresponding to its energy E_γ, for any detector type. This method can be used to calibrate cylindrical, well-type, and parallelepiped scintillation and semi-conductor detectors for isotropic radiating gamma-ray (point, plane and volumetric) sources. Recently, Abbas [8–10] introduced a new approach involving the determination of the path length $d(\theta,\varphi)$, covered by a photon inside the detector active volume and the geometrical solid angle Ω (the angle subtended by the detector at the source point) for 4π NaI(Tl), and cylindrical (phoswich and lanthanum bromide) scintillation detectors by using a direct mathematical formula.

Moens et al. [11, 12] calculated the detector efficiency based on the efficiency transfer principle using a new straightforward analytical definition to compute the effective solid angle between the source and the detector. The attenuation of photons by the source-detector system was considered and determined. They calculated the full-energy peak efficiency of cylindrical gamma detectors using different source geometries, i.e. point, disk and cylindrical shaped sources. Full account is taken of gamma attenuation in the source and in any absorbing layer. Also, they presented a new method to calculate with improved accuracy the absolute peak efficiency of cylindrical Ge(Li) detectors.

Piton et al. [13] used ETNA program to determine the detector efficiency using the efficiency transfer principle for various types of sources for coaxial source-detector geometries and coincidence summing corrections. Badawi et al. [14] calculated the full energy peak efficiency of scintillation detector using an empirical formula based on experimental measurements of axial cylindrical sources based on the ratio of the source detector solid angle with the source self-absorption effect taken into account. Thabet et al. [15] calculated the detector's efficiency for NaI scintillation detectors using ANGLE 4 software, that based also on efficiency transfer principle.

In this work we use a simple analytical method to calculate the full-energy peak efficiency of the cubic NaI(Tl) gamma-ray detector with a well-rectangular cavity. The analytical method considers the source-to-detector distance, the distance traveled by photons inside the detector active mediums and the effective solid angle ratio. The rectangular-well cavity detector design is considered because it may accept samples of different shapes than that of a regular cylindrical-well detector. This can be useful in several biological, environmental and neutron activation analysis techniques. The numerical trapezoidal method was used to solve the analytical equations, the outcomes were compared with the laboratory results and Geant4 Monte Carlo simulation code, which shows a good agreement for the both methods with the applied analytical method.

2 Mathematical viewpoint

Determination of the effective solid angle between the source and the detector active medium is very important for determining the detector efficiency. All the possible path-lengths inside the detector active medium and all absorbers between them must be considered. The effective solid angle is defined by [8–10] as:

$$\Omega_{\text{eff}} = \int_{\theta}\int_{\phi} f_{\text{att}}.f.\sin\boldsymbol{\theta}\, d\theta d\phi \tag{2.1}$$

Where f and f_{att} factors are expressed as:

$$f = \left(1 - e^{-\mu d}\right) \& f_{\text{att}} = e^{-\sum_{i=1}^{n} \mu_i \delta_i} \tag{2.2}$$

Here, d is the path-length travelled by the photon through the detector crystal, μ_i is the attenuation coefficient of the i^{th} absorber (Al end- cap, Alminum oxide Reflector and Plexiglass holder) for a gamma-ray photon with energy E_γ [16], and δ_i is the gamma-photon path-length through the i^{th} absorber and it can be defined as the following.

$$\begin{aligned} \delta_i &= \left(\frac{t_i}{\cos\theta}\right) \text{For the horizontal absorber layers, or} \\ \delta_i &= \left(\frac{t_i}{\sin\theta}\right) \text{For the vertical absorber layers.} \end{aligned} \tag{2.3}$$

2020 JINST 15 P02013

where t_i is the thickness of the absorber layer. The efficiency transfer method offers a solution to the problems encountered in the experimental measurements. It can be used to calculate the efficiency of the detector using any geometrical parameters of the source and the detector depending on the ratio of the effective solid angles, according to the following equation [17–21]:

$$\varepsilon_{target} = \frac{\Omega_{target}}{\Omega_{ref}} \varepsilon_{ref} \tag{2.4}$$

where, ε_{target} and ε_{ref}, are the full-energy peak efficiencies of the target and the reference geometry, respectively. Ω_{target} and Ω_{ref} are the effective solid angles subtended by the detector surface with the target and the reference point-like source, respectively. The axially positioned radioactive point-like source that placed at a distance, h, from the detector surface is shown in figure 1.

The probability of the path-lengths of the photons which enter in the detector must be known in order to calculate the effective solid angle, Ω_{eff}, of the source-to-detector system. Knowing the effective solid angle, the detecting efficiency can be calculated, using the efficiency transfer principle. From figure 1, the direction of the incident photon is defined by the polar θ and azimuthal ϕ angles; the azimuthal angle ϕ takes the value from 0 to 2π, while the polar angle θ is determined from the following four different expressions that depend on the source-detector configuration.

$$\begin{aligned} \theta_1 &= \tan^{-1}\left(\frac{m}{h+S}\right) \quad \text{and } \theta_2 = \tan^{-1}\left(\frac{m}{h}\right) \quad \text{where, } m = \frac{a}{\cos(\theta)} \\ \theta_3 &= \tan^{-1}\left(\frac{M}{2L+h}\right) \quad \text{and } \theta_4 = \tan^{-1}\left(\frac{M}{h}\right) \quad \text{where, } M = \frac{L}{\cos\theta} \end{aligned} \tag{2.5}$$

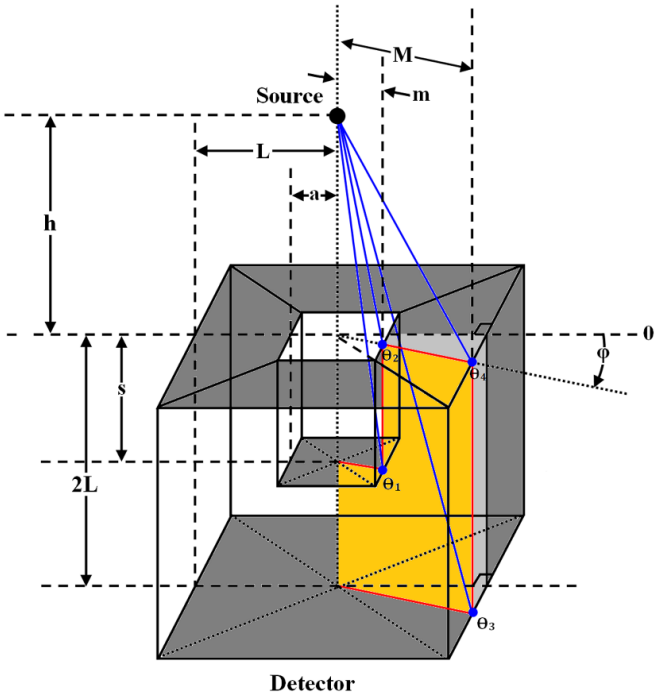

Figure 1. Schematic diagram of the cubic detector with rectangular cavity with axially positioned radioactive point-like source, placed outside the detector cavity.

Here, 2L is the length of the detector, 2a is the width of the cavity; S is the cavity depth. According to the source-detector geometry, shown in figure 2, there are three different cases to represent the effective solid angle Ω_{eff}: the first case — $\theta_4>\theta_3>\theta_2>\theta_1$, the second case — $\theta_4>\theta_2>\theta_3>\theta_1$ and the third case — $\theta_4>\theta_2>\theta_1>\theta_3$. Each case relies upon the separation distance between the source and the detector. When the radioactive point-like source is placed axially outside the cubic detector cavity, the photons have six possible paths-lengths to enter and leave the detector active medium depending on the polar angles. These path-lengths are calculated by the equations (2.6) and are shown in figure 2:

$$\begin{aligned} d_1 &= \frac{2L - s}{\cos\theta} & d_4 &= \frac{M - m}{\sin\theta} \\ d_2 &= \frac{M}{\sin\theta} - \frac{s}{\cos\theta} & d_5 &= \frac{2L}{\cos\theta} \\ d_3 &= \frac{2L}{\cos\theta} - \frac{m}{\sin\theta} & d_6 &= \frac{M}{\sin\theta} - \frac{h}{\cos\theta} \end{aligned} \tag{2.6}$$

a. Case 1: $\theta_4>\theta_3>\theta_2>\theta_1$. Only four possible paths-lengths have been found (d_1,d_3, d_5, and d_6) and the effective solid angle Ω_{eff} is calculated by the following equation:

$$\Omega_{eff} = 8\int_0^{\frac{\pi}{4}} \left[\int_0^{\theta_1} f_{att} f_1 \, sin\theta d\theta + \int_{\theta_1}^{\theta_2} f_{att} f_3 \, sin\theta d\theta + \int_{\theta_2}^{\theta_3} f_{att} f_5 \, sin\theta d\theta + \int_{\theta_3}^{\theta_4} f_{att} f_6 \, \sin\theta d\theta \right] d\varphi \tag{2.7}$$

where $f_i = \left(1 - e^{-\mu.d_i}\right)$, for i = 1, 3, 5 and 6

b. Case 2: $\theta_4>\theta_2>\theta_3>\theta_1$. Only four possible paths-lengths have been found (d_1,d_3, d_4, and d_6) and the effective solid angle Ωeff is calculated by the following equation:

$$\Omega_{eff} = 8\int_0^{\frac{\pi}{4}} \left[\int_0^{\theta_1} f_{att}.f_1 \, \sin\theta d\theta + \int_{\theta_1}^{\theta_3} f_{att}.f_3 \, \sin\theta d\theta + \int_{\theta_3}^{\theta_2} f_{att}.f_4 \, \sin\theta d\theta + \int_{\theta_2}^{\theta_4} f_{att}.f_6 \, \sin\theta d\theta \right] d\varphi \tag{2.8}$$

where $f_i = \left(1 - e^{-\mu.d_i}\right)$, for i = 1, 3, 4 and 6

c. Case 3: $\theta_4>\theta_2>\theta_1>\theta_3$. Only four possible paths-lengths have been found (d_1, d_2, d_4, and d_6) and the effective solid angle Ω_{eff} is calculated by the following equation:

$$\Omega_{eff} = 8\int_0^{\frac{\pi}{4}} \left[\int_0^{\theta_3} f_{att}.f_1 \, \sin\theta d\theta + \int_{\theta_3}^{\theta_1} f_{att}.f_2 \, \sin\theta d\theta + \int_{\theta 1}^{\theta_2} f_{att}.f_4 \, \sin\theta d\theta + \int_{\theta_2}^{\theta_4} f_{att}.f_6 \, \sin\theta d\theta \right] d\varphi \tag{2.9}$$

where $f_i = \left(1 - e^{-\mu.d_i}\right)$, for i = 1, 2, 4 and 6

2020 JINST 15 P02013

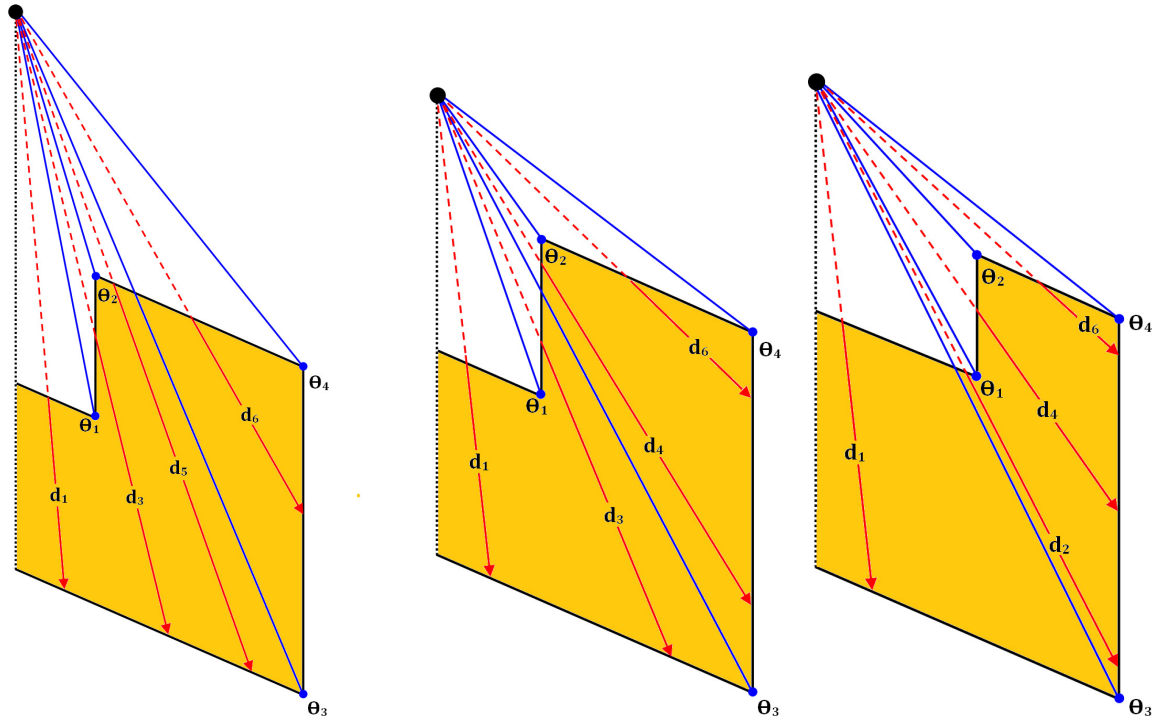

(a) a. Case 1: $\theta_4 > \theta_3 > \theta_2 > \theta_1$. **(b)** b. Case 2: $\theta_4 > \theta_2 > \theta_3 > \theta_1$. **(c)** c. Case 3: $\theta_4 > \theta_2 > \theta_1 > \theta_3$.

Figure 2. The three possible cases of the axial point-like source, placed outside the cubic detector cavity.

3 Geant4 simulation

In Geant4 are accounted the all electro-magnetic interactions of gamma-rays with the detecting media. In Geant4 a library of electro-magnetic interaction of low energy has been created [22] and the valid energy range is extended down to 250 eV. This improvement is based on the use of experimental data parameterizations utilizing the databases created by the Lawrence Livermore National Laboratory (LLNL): EPDL97 (Evaluated-Photon-Data-Library), EEDL (Evaluated-Electron-Data-Library) and EADL (Evaluated-Atomic-Data-Library). This low limit, together with the available in Geant4 physical processes, allows us to use Geant4 for simulating the energy response of the cubic scintillation detector. The energies which are used for simulated program are tabulated in table 1, which are the same energy used experimentally and mathematically. The configuration of the simulated cubic detector with rectangular cavity and Geant4 generated a gamma-photons are shown in figure 3.

4 Experimental setup

4.1 Radioactive sources

The calibration process and experimental measurements were done using four radioactive standard point-like sources, which were purchased from the Physikalisch Technische Bundesanstalt (PTB) in Braunschweig and Berlin. The four point-like sources, ^{137}Cs, ^{60}Co, ^{133}Ba and ^{152}Eu, cover an energy range from 80.99 keV to 1408.01 keV. The half-life, photon energies and the probabilities

2020 JINST 15 P02013

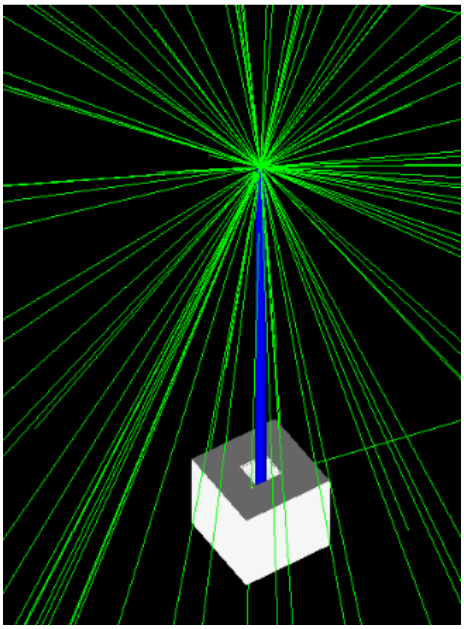

Figure 3. Geant4 simulation of the cubic detector with rectangular cavity and axially positioned radioactive point-like source.

of photon emission per decay for all radionuclides used in the calibration process and its activities tabulated in table 1.

Table 1. Point sources activities and their half lives, photon energies and photon emission probabilities per decay.

Nuclide	Energy (keV)	Emission Probability %	Half Life (Days)	Activity (kBq) on 1 June 2009
^{133}Ba	80.99	34.10	3847.91	275.3
^{152}Eu	121.78	28.40	4943.29	290.0
	244.69	7.49		
	344.28	26.60		
	964.13	14.00		
	1408.01	20.87		
^{137}Cs	661.66	85.21	11004.98	385.0
^{60}Co	1173.20	99.90	1925.31	212.1
	1332.50	99.98		

4.2 Gamma detector

The cubic gamma-ray NaI(Tl) scintillation detector with rectangular cavity was purchased from Saint-Gobain Crystals, based on Special Order from Radiation Physics Laboratory, Faculty of

2020 JINST 15 P02013

Science, Alexandria University, Egypt. The manufacturer drawing of the detector with rectangular cavity is illustrated in figure 4.

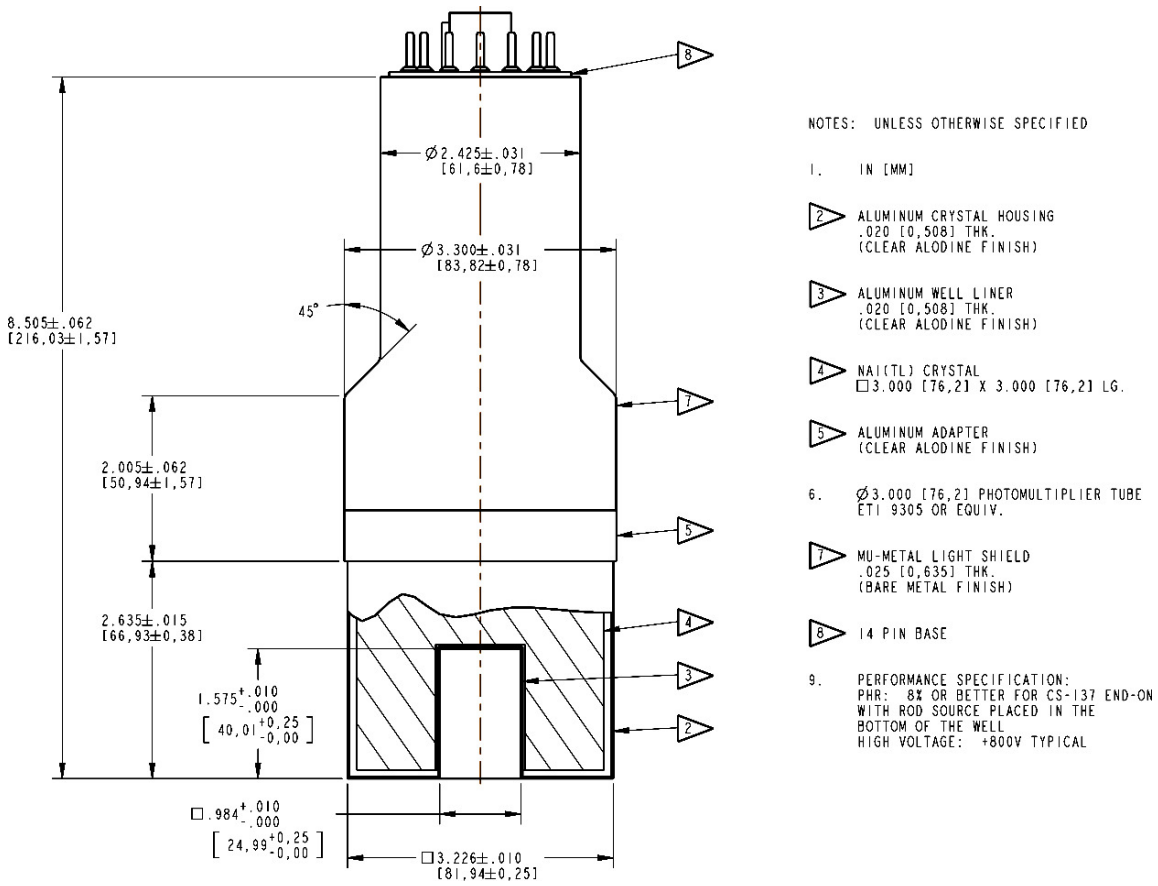

Figure 4. Manufacturer drawing of specially ordered cubic detector with rectangular cavity.

4.3 Experimental efficiency determination

The experimental efficiency values ε for a given photon energy is obtained using the following formula:

$$\varepsilon = \frac{N}{TP_{\gamma}AC_d} \tag{4.1}$$

where,

$$C_d = e^{-\lambda T} . \tag{4.2}$$

N, is the total number of counts in the full energy peak, T(s) is the elapsed time, P_γ is the probability of a photon emission [23], A(Bq) is the activity of radionuclide and C_d is the correction factor due to radionuclide decay as a function of the decay constant $\lambda(s^{-1})$. The measuring time was sufficiently long in order to obtain a net peak area uncertainty less than 0.5%. Additionally, background subtraction was performed where The first step in the library locate phase is determination of the continuum background. This is done by "erosion" process that effectively smoothes that spectrum. At the end of this process, the resulting background spectrum is subtracted

from the original spectrum to form a net spectrum. Dead time values were found to be less than 1 % in all measured spectra; therefore, no correction for the dead time was done. The measurements of the four standard sources were done at separation distances of 21.5 cm, 29.5 cm and 37.0 cm, measured from the detector surface, to avoid the coincidence-summing effect. The full energy peak efficiency of radionuclides was measured at 37.0 cm, which was considered to be a reference position. This reference position efficiency was used to transfer it to the other two positions. All radioactive point-like sources were measured with the help of a homemade Plexiglas holder of two horizontal layers, the first (3.68 mm-thick) is the base of the support that is placed directly on the top of the detector, the second Plexiglas layer (2.55 mm-thick) is placed below the radioactive source as a holder.

5 Results

The experimental values of the full energy peak efficiency at the reference position with their uncertainties are shown in table 2. The effective solid angles at 21.5 cm, 29.5 cm and 37.0 cm were calculated as presented in section 2. Also, the calculated values of the full energy peak efficiency were obtained by using equation 4. The relative deviation percentage $(R_D\%)_1$ between the experimental and calculated full energy peak efficiency are determined according to the formula (5.1) and the values are shown in tables 3 and 4:

$$(R_D\%)_1 = \frac{\varepsilon_{Calc} - \varepsilon_{exp}}{\varepsilon_{exp}} \times 100 \tag{5.1}$$

The mean discrepancy of ~5% between the experimental and calculated full energy peak efficiency is found to be acceptable.

According to figures 5 and 6, and the data listed in tables 3 and 4, there is an agreement between the experimental values and simulated ones, obtained by means of Geant4. The results are in good agreement at both low- and high- energy regions.

The relative deviation percentage $(R_D\%)_2$ values between the experimental and Geant4 simulated full energy peak efficiency are determined according to the following equation:

$$(R_D\%)_2 = \frac{\varepsilon_{GEANT4} - \varepsilon_{exp}}{\varepsilon_{exp}} \times 100 \tag{5.2}$$

6 Conclusions

In the present work, a new analytical method based on the source-to- detector geometry, calculation of the distance traveled by gamma-ray within the detector materials, and the effective solid angle ratio, was used to calculate the full-energy peak efficiency of the well-cubic NaI(Tl) gamma-ray detector for axially positioned sources outside of the well-cavity. Experimental measurements using radioactive point sources, located out the detector cavity at different heights were performed to evaluate the performance of this new method. A computer program was developed to solve the analytical model and validated it with laboratory results and Geant4 Monte Carlo code. Results based on this setup indicate good agreement between the measured full-energy peak efficiency values, those simulated using Geant4, and the predictions of the analytical model. These programmed

2020 JINST 15 P02013

Table 2. The full energy peak efficiency at the reference position of 37.0 cm separation distance and their uncertainties.

Nuclide	*Energy (keV)*	*Experimental Efficiency*	*Experimental Efficiency Uncertainty*
Ba-133	80.99	2.66E-03	1.86E-05
Eu-152	121.78	2.89E-03	2.40E-05
Eu-152	244.69	1.98E-03	2.26E-05
Eu-152	344.28	1.49E-03	1.22E-05
Cs-137	661.66	9.62E-04	1.06E-05
Eu-152	964.13	6.49E-04	7.62E-06
Co-60	1173.23	6.34E-04	4.86E-06
Co-60	1332.50	5.84E-04	4.42E-06
Eu-152	1408.01	5.80E-04	5.27E-06

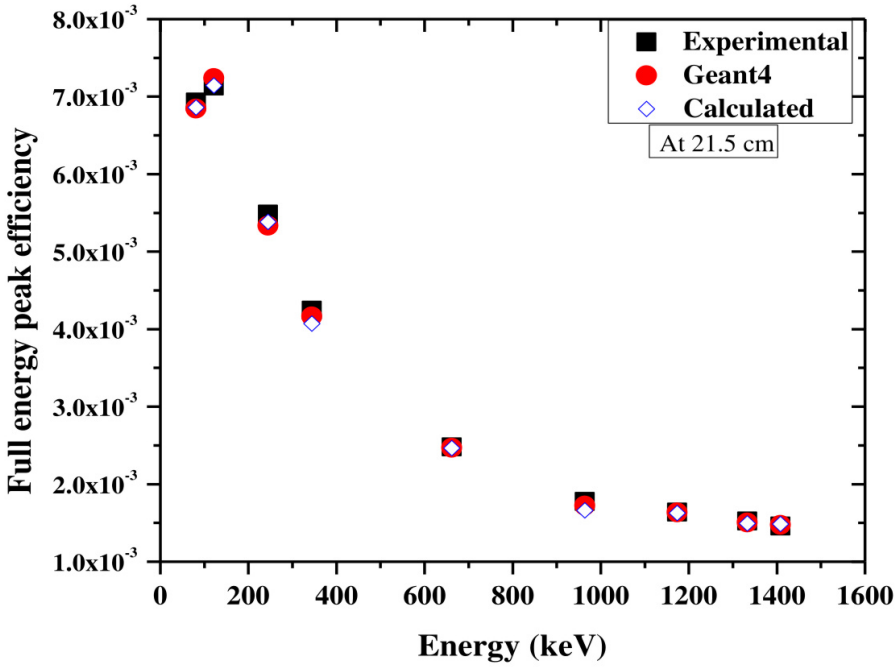

Figure 5. Experimental, theoretical and Geant4 simulation full energy peak efficiency at 21.5 cm separation distance.

mathematical methods are a very simple and fast calculation procedure for the calculation process, especially in case of extended sources. In future work we will explore the viability of application to distributed sources.

2020 JINST 15 P02013

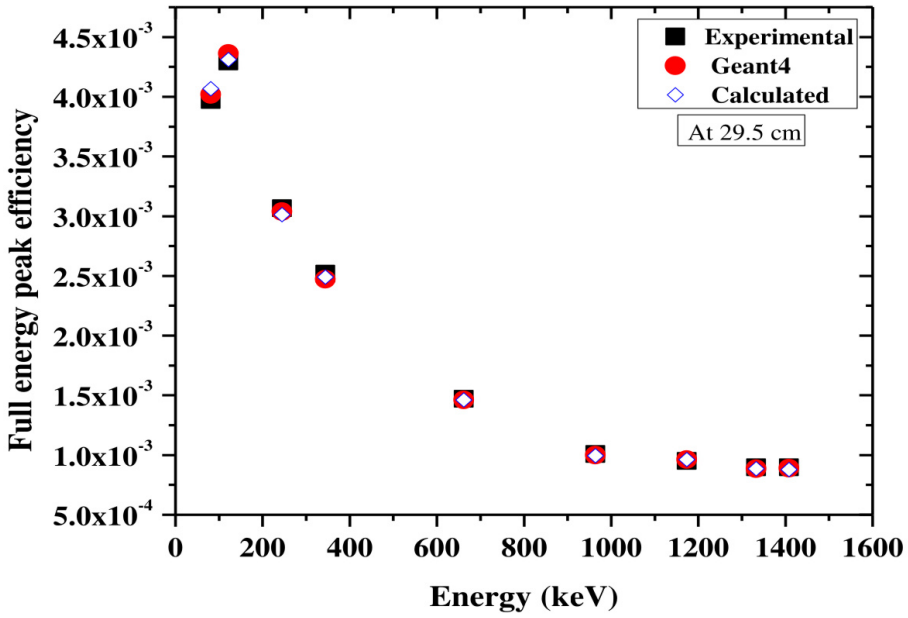

Figure 6. Experimental, theoretical and Geant4 simulation full energy peak efficiency at 29.5 cm separation distance.

Table 3. Determined efficiencies and their relative deviation percentages at 21.5 cm separation distance from the detector surface.

Nuclide	*Energy (keV)*	ε_{exp}	ε_{Calc}	$(R_D\%)_1$	ε_{Geant4}	$(R_D\%)_2$
Ba-133	80.99	6.93E-03	6.86E-03	-1.01%	6.84E-03	-1.30%
Eu-152	121.78	7.14E-03	7.14E-03	0.00%	7.24E-03	1.40%
Eu-152	244.69	5.48E-03	5.38E-03	-1.82%	5.33E-03	-2.74%
Eu-152	344.28	4.24E-03	4.07E-03	-4.01%	4.16E-03	-1.89%
Cs-137	661.66	2.48E-03	2.47E-03	-0.40%	2.47E-03	-0.40%
Eu-152	964.13	1.78E-03	1.69E-03	-5.06%	1.72E-03	-3.37%
Co-60	1173.23	1.64E-03	1.63E-03	-0.61%	1.63E-03	-0.61%
Co-60	1332.50	1.53E-03	1.50E-03	-1.96%	1.51E-03	-1.31%
Eu-152	1408.01	1.46E-03	1.48E-03	1.37%	1.47E-03	0.68%

Acknowledgments

This work was done in the frame of the protocol for Joint Scientific Research, sighed between Frank Laboratory of Neutron Physics (FLNP) of the Joint Institute for Nuclear Research (JINR) in Dubna, Russian Federation and Alexandria University in Alexandria, Egypt.

2020 JINST 15 P02013

Table 4. Determined efficiencies and their relative deviation percentages at 29.5 cm separation distance from the detector surface.

Nuclide	*Energy (keV)*	ε_{exp}	ε_{Calc}	$(R_D\%)_1$	ε_{Geant4}	$(R_D\%)_2$
Ba-133	80.99	3.97E-03	4.07E-03	2.52%	4.02E-03	1.26%
Eu-152	121.78	4.29E-03	4.31E-03	0.47%	4.36E-03	1.63%
Eu-152	244.69	3.07E-03	3.01E-03	-1.95%	3.04E-03	-0.98%
Eu-152	344.28	2.52E-03	2.49E-03	-1.19%	2.47E-03	-1.98%
Cs-137	661.66	1.47E-03	1.46E-03	-0.68%	1.46E-03	-0.68%
Eu-152	964.13	1.01E-03	9.95E-04	-1.49%	9.98E-04	-1.19%
Co-60	1173.23	9.50E-04	9.63E-04	1.37%	9.61E-04	1.16%
Co-60	1332.50	8.96E-04	8.86E-04	-1.12%	8.86E-04	-1.12%
Eu-152	1408.01	8.98E-04	8.79E-04	-2.12%	8.89E-04	-1.00%

References

[1] L. Moens et al., *Calculation of the absolute peak efficiency of gamma-ray detectors for different counting geometries*, *Nucl. Instrum. Meth.* **187** (1981) 451.

[2] D. Karamanis, V. Lacoste, S. Andriamonje, G. Barreau and M. Petit, *Experimental and simulated efficiency of a HPGe detector with point-like and extended sources*, *Nucl. Instrum. Meth.* **A 487** (2002) 477.

[3] GEANT4 collaboration, *GEANT4: a simulation toolkit*, *Nucl. Instrum. Meth.* **A 506** (2003) 250.

[4] J. Allison et al., *GEANT4 developments and applications*, *IEEE Trans. Nucl. Sci.* **53** (2006) 270.

[5] Y.S. Selim and M.I. Abbas, *Source-detector geometrical efficiency*, *Radiat. Phys. Chem.* **44** (1994) 1.

[6] Y.S. Selim and M.I. Abbas, *Direct calculation of the total efficiency of cylindrical scintillation detectors for extended circular sources*, *Radiat. Phys. Chem.* **48** (1996) 23.

[7] Y.S. Selim and M.I. Abbas, *Analytical calculations of gamma scintillators efficiencies. II. Total efficiency for wide coaxial circular disk sources*, *Radiat. Phys. Chem.* **58** (2000) 15.

[8] M.I. Abbas, *Analytical approach to calculate the efficiency of 4π NaI(Tl) gamma-ray detectors for extended sources*, *Nucl. Instrum. Meth.* **A 615** (2010) 48.

[9] M.I. Abbas, *A new analytical method to calibrate cylindrical phoswich and $LaBr_3(Ce)$ scintillation detectors*, *Nucl. Instrum. Meth.* **A 621** (2010) 413.

[10] M.I. Abbas, *Analytical formulae for borehole scintillation detectors efficiency calibration*, *Nucl. Instrum. Meth.* **A 622** (2010) 171.

[11] L. Moens et al., *Calculation of the absolute peak efficiency of gamma-ray detectors for different counting geometries*, *Nucl. Instrum. Meth.* **187** (1981) 451.

[12] L. Moens et al., *Calculation of the absolute peak efficiency of Ge and Ge(Li) detectors for different counting geometries*, *J. Radioanal. Chem.* **70** (1982) 539.

2020 JINST 15 P02013

[13] F. Piton, M.-C. Lépy, M.-M. Bé and J. Plagnard, *Efficiency transfer and coincidence summing corrections for γ-ray spectrometry*, *Appl. Radiat. Isot.* **52** (2000) 791.

[14] M.S. Badawi, A.M. El-Khatib, M.A. Elzaher, A.A. Thabet and A.A. Saker, *Using an analytical efficiency transfer principle to calculate the full energy peak efficiency for gamma detectors*, *Vestnik Orenburg State Univ.* **05** (154) 164.

[15] A. Thabet et al., *Experimental verification of gamma-efficiency calculations for scintillation detectors in ANGLE* 4 *software*, *Nucl. Technol. Radiat. Protect.* **30** (2015) 35.

[16] J.H. Hubbell and S.M. Seltzer, *Tables of X-ray mass attenuation coefficients and mass energy-absorption coefficients*, National Institute of Standards and Technology, Gaithersburg, MD, U.S.A. (1995).

[17] M.M. Gouda et al., *Calibration of well-type NaI(Tl) detector using a point sources measured out the detector well at different axial distances*, 2015 *JINST* **10** P03022.

[18] A.M. El-Khatib et al., *Well-type NaI(Tl) detector efficiency using analytical technique and ANGLE* 4 *software based on radioactive point sources located out the well cavity*, *Chin. J. Phys.* **54** (2016) 338.

[19] M.S. Badawi, M. Abd-Elzaher, A.A. Thabet and A.M. El-Khatib, *An empirical formula to calculate the full energy peak efficiency of scintillation detectors*, *Appl. Radiat. Isot.* **74** (2013) 46.

[20] A.M. El-Khatib, A.A. Thabet, M.A. Elzaher, M.S. Badawi and B.A. Salem, *Study on the effect of the self-attenuation coefficient on γ-ray detector efficiency calculated at low and high energy regions*, *J. Nucl. Ener. Sci. Technol.* **46** (2014) 217.

[21] M.M. Gouda et al., *Mathematical method to calculate full-energy peak efficiency of detectors based on transfer technique*, *Indian J. Phys.* **90** (2015) 201.

[22] S. Giani et al., *GEANT simulation of energy losses of slow hadrons*, CERN-OPEN-99-121, CERN, Geneva, Switzerland (1999) [INFN-AE-99-20] [INFN-AE-99-21].

[23] R.B. Firestone, *Table of isotopes*, 8th edition, Wiley, New York, NY, U.S.A. (1996).

2020 JINST 15 P02013